Electronic Structures and Vibrational Properties of a Carbon Nanotube with Adsorption of Small Hydrocarbon Radicals

ARTICLE *in* THE JOURNAL OF PHYSICAL CHEMISTRY C · NOVEMBER 2008

Impact Factor: 4.77 · DOI: 10.1021/jp806265q

2 AUTHORS, INCLUDING:

H. Y. He
University of Science and Technology of C…

37 PUBLICATIONS **189** CITATIONS

SEE PROFILE

Article

Electronic Structures and Vibrational Properties of a Carbon Nanotube with Adsorption of Small Hydrocarbon Radicals

H. Y. He, and B. C. Pan

J. Phys. Chem. C, **2008**, 112 (48), 18876-18881• DOI: 10.1021/jp806265q • Publication Date (Web): 07 November 2008

Electronic Structures and Vibrational Properties of a Carbon Nanotube with Adsorption of Small Hydrocarbon Radicals

H. Y. He* and B. C. Pan

Hefei National Laboratory for Physical Sciences at Microscale and Department of Physics, University of Science and Technology of China, Hefei, Anhui 230026, People's Republic of China

Received: July 15, 2008; Revised Manuscript Received: September 24, 2008

We employ density functional theory to investigate electronic structures and vibrational properties of a (7,0) carbon nanotube with adsorption of CH, CH_2, or CH_3 on the outer wall. We find that the edge states or gap states are induced in the band structure by the adsorption of CH, CH_2, or CH_3. This predicts that a carbon nanotube can be functionalized by the adsorbed radicals. Furthermore, the calculated vibrational density of states shows that, apart from the common C−H stretching and bending modes, each adsorbed radical introduces new vibrational modes, such as the swing modes, in the low frequency region below 500 cm^{-1}. In addition, different numbers and different frequencies of the stretching modes for the radicals can be used to identify the adsorbed radicals each other.

I. Introduction

Carbon nanotubes (CNTs) can adsorb many different kinds of species, such as molecules, metals, and radicals, on the outer walls[1−15] which is the so-called surface decoration of the CNTs. So far, it has been realized that such decoration is a promising way to modulate the physical and chemical properties of the carbon nonatubes. For instance, in experiment, when a carbon nanotube was exposed to air and oxygen,[2] the adsorbed species influenced the tube's electronic resistance and local density of states dramatically. On the theoretical side, the transport properties of single walled carbon nanotube bundles were also predicted to be quite sensitive to the attached N_2, He,[16] hydrogen atoms,[7] water,[6,10] and so on.

Recently, it was found experimentally that small hydrocarbon radicals (CH, CH_2, and CH_3) could adsorb on the outer walls of CNTs.[17] Most probably, the adsorption of the radicals changes the electronic structures of the tubes. Such changes may depend on the kind of the radical as well as on the adsorption sites in the tubes. Systematic investigation of electronic structures of these concerned cases is significant to understand the interaction of a radical with a carbon nanotube and for the potential application of the CNTs.

On the other hand, previous theoretical works[18,19] revealed that, in the defect free region of a tube, CH and CH_2 energetically prefer to adsorb on the centers of the bonds parallel to the tube axis and CH_3 on the top site of a carbon atom, with energy cost of less than 0.9 eV. In contrast, the radicals can all adsorb on the dangling bond (DB) atom at a single vacancy in a tube spontaneously. Moreover, it was predicted that, driven by temperature effect, these radicals not only diffuse on the outer wall of the tube with different behaviors, but also can heal the single atomic vacancies in the tube undergoing different atomistic processes.

Basically, such different behaviors and atomistic processes are attributed to the different structural features of the radicals locating at the favored sites in the defect-free region or at the DB atom in a vacancy. Definitely, the structural features reflect on the vibrational frequencies that are usually regarded as fingerprint of each system. Thus, evaluating the vibrational frequencies of the radicals depositing at the favored sites in CNT can provide direct indicators, which can be compared with experimental vibrational spectra in future.

In this paper, we investigate the electronic and vibrational properties of CH, CH_2, or CH_3 adsorbed either in the defect free region or on a single vacancy in a carbon nanotube by performing the density functional theory (DFT) calculation. We find that the electronic structures of a carbon nanotube are modified by the adsorption of each radical. Moreover, our calculations show evidently that apart from the stretching modes and bending modes of C−H bonds, new vibrational features, swing modes, appear in the low frequency region. In addition, according to our calculations, the different numbers and frequencies of the C−H stretching modes for the adsorbed radicals can differ the adsorbed radicals from each other.

II. Computational Method

Our calculations are performed by using the SIESTA program,[20] where the norm-conserving pseudopotential and the Perdew−Burke−Ernzerhof generalized gradient approximation (GGA-PBE)[21] are considered. Double-ζ basis sets[22] are used for C and H atoms, and spin polarization is taken into account in our calculations. There are various sized carbon nanotubes available for calculations. In our calculations, we focus on the electronic as well as the vibrational properties of a carbon nanotube with adsorption of different hydrocarbon radicals. For such complex systems, the supercells should be used. As a result, the computational demand in vibrational calculations at the level of density functional theory is huge if the size of the supercell is not small. To practice our calculation, we have to select a carbon nanotube with a proper size. So, the (7,0) carbon nanotube was selected for our calculations. Here, the zigzag (7,0) carbon nanotube with or without a single vacancy is taken into account, on which CH, CH_2, and CH_3 adsorb respectively. A periodic boundary condition along the tube axis is applied for each system. The supercell length in the tube axis is set to be 25.56 Å, which is large enough to neglect the interaction between the adsorbates and their images. For such a large supercell, the Brillouin zone is sampled with a set of *k*-point

* To whom correspondence should be addressed.

10.1021/jp806265q CCC: $40.75
Published on Web 11/07/2008

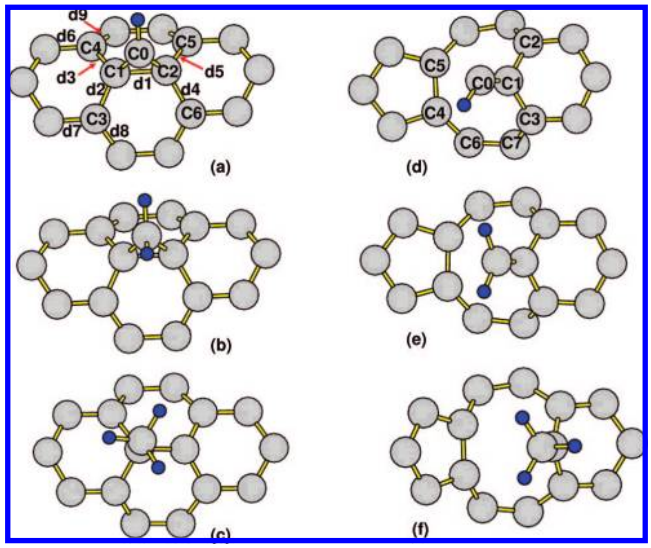

Figure 1. (Color online) The local configurations of CH (a), CH_2 (b), and CH_3 (c) adsorbed in the perfect network and CH (d), CH_2 (e), and CH_3 (f) adsorbed at the dangling bond atom in a (7,0) tube. The blue balls stand for H atoms, and the gray balls indicate C atoms. The typical atoms and bonds are labeled with characters in (a) and (d). Both (b) and (c) refer to the same typical atoms and bonds marked in (a), and both (e) and (f) to (d).

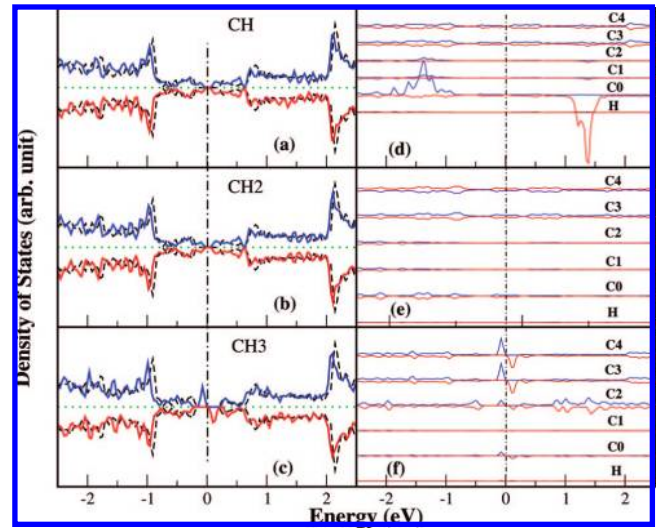

Figure 2. Total electronic density of states for (a) CH, (b) CH_2, and (c) CH_3 in the perfect network of (7,0) tube, and the local density of states for (d) CH, (e) CH_2, and (f) CH_3 adsorption. The labeled characters in (d−f) refer to the atoms marked in Figure 1. The majority spin states and the minority spin states are shown with blue and red solid lines, upper and below, respectively. The black dashed lines in (a−c) stand for the total density of states of the perfect (7,0) tube. The dot-dash lines indicate the Fermi levels, which are shifted to zero.

grid ($1 \times 1 \times 10$) according to the Monkhorst−Pack scheme.[23] Here our test calculation shows that the ($1 \times 1 \times 10$) k-point grid is enough for our calculations about the concerned systems. We employ the frozen phonon approximation[24] to calculate the vibrational frequencies of the concerned systems. The atoms in each system are displaced with an amplitude of 0.04 Bohr one by one from their equilibrium positions along three Cartesian directions and the reverse directions. By the numerical derivatives for the displacements of each atom, the force constants are obtained. These force constants are used to build up the dynamical matrix of the systems. By solving the dynamical equation

$$\omega^2 M_i u_{i,\alpha} = \sum_{j,\beta} C_{i,\alpha;j,\beta} u_{j,\beta} \quad (1)$$

the zone-center vibrational frequencies ω and the corresponding eigenmodes $u_{i,\alpha}$ are yielded, where the M_i is the mass of the ith atom, $C_{i,\alpha;j,\beta}$ is the force constant, and α (β) means the direction of x, y, or z.

III. Results and Discussions

A. Electronic Structures. First, we fully relax the geometries of a (7,0) tube with or without a single vacancy, with the residual force convergence value being less than 0.02 eV/Å. Similar to the previous report,[25] the configuration of the relaxed single vacancy in the (7,0) tube converts to be a dangling bond atom and a pentagon, which is termed as a 5−1DB defect. Then we put each radical on the perfect network and on the DB atom of the tube, respectively. In the perfect region of the tube, the energetically preferable adsorption site for either CH or CH_2 is found to be the center of a C−C bond parallel to the tube axis. This is due to the fact that both CH and CH_2 have more than one dangling bond, so they prefer to bond with two atoms, whereas for CH_3, with one dangling bond, its favorite adsorption site is atop site of a C atom in the CNT. The local configurations for the radicals adsorbing both in the defect-free region and on the DB atom are shown in Figure 1, where some typical atoms and bonds in (a) and (d) are labeled with characters, and those in (b) and (c) and (e) and (f) refer to (a) and (d) respectively.

For these configurations, we calculate their electronic density of states. It shows clearly in Figure 2 that the adsorbed radicals alter the electronic structure of the pure tube, especially near the band edges, where the majority spin states (upper) and the minority spin states (lower) are plotted separately. For the CH or CH_2 adsorption, the local states appear near the edges of valence band and conduction band. For the CH_3 adsorption, we observe two peaks at −0.1 eV (majority spin state) and +0.1 eV (minority spin state) with respect to the Fermi level (E_f).

To go further, we calculate the local density of states (LDOS) for each case. As shown in Figure 2d, the edge states in the case of CH mainly come from the contribution of C3 and C4, as well as their equivalent atoms, C6 and C5 (marked in Figure 1a), in which only C3 and C4 are plotted as examples. This is due to the fact that, with adsorption of CH, the carbon atoms of C1 and C2 undergo the transition from sp^2 to sp^3 hybridization, with the occurrence of longer bonds of d1, d2, d3, and d4 (1.50 Å) and shorter bonds of d6, d7, d8, and d9 (1.40 Å) around C3, C4, C5, and C6 atoms (see Figure 1a). Generally, the strained bonds may create new bonding states and antibonding states. The eigenvalues corresponding to the new antibonding states distribute mainly around the conduction band edge and that of the new bonding states around the valence band edge, of which some new antibonding states position below the conduction band edge, and some new bonding states are above the valence band edge. Thus, the strained bonds not only make the change of the DOS shape but also cause the edge states near the band gap. Such a situation is observed in our calculations. In addition, we find several pronounced resonant states caused by C0 at about 1.4 eV below or above the Fermi level. Essentially, such resonant states are associated with the feature of the local atomic structure around the C0 atom: connecting with two carbons and a H atom, C0 characterizes sp^3 like hybridization, resulting in an unpaired electron in C0. In other wards, there exists a dangling bond in the C0 atom, which is responsible for these local states.

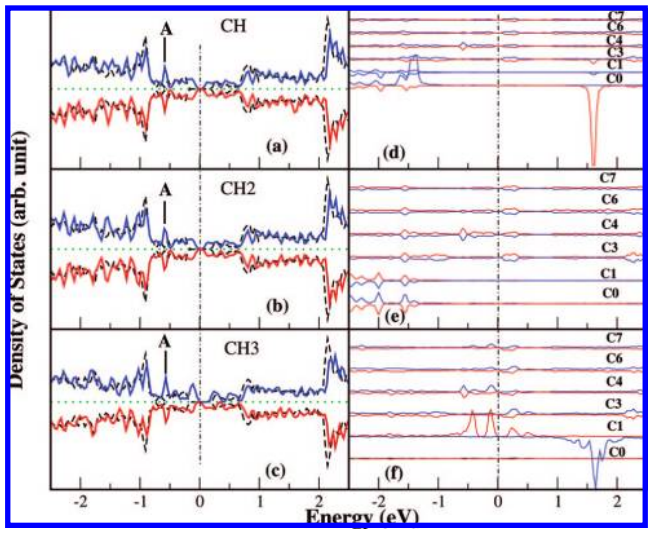

Figure 3. Total electronic density of states for (a) CH, (b) CH_2, and (c) CH_3 at the dangling bond atom in (7,0) tube, and the local density of states for (d) CH, (e) CH_2, and (f) CH_3 adsorption. The labeled characters in (d−f) refer to the atoms marked in Figure 1. The majority spin states and the minority spin states are shown with blue and red solid lines, upper and below, respectively. The black dashed lines in (a−c) stand for the total density of states of the perfect (7,0) tube. The dot−dash lines indicate the Fermi levels, which are shifted to zero.

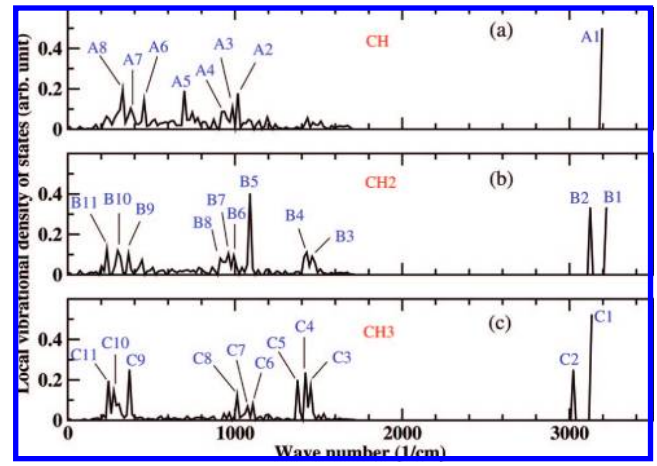

Figure 4. Local vibrational density of states for the radicals on the (7,0) tube. Some typical peaks are marked with characters.

For the case of CH_2, the local geometry around the adsorption site (seen in Figure 1b) is similar to that of CH (Figure 1a). So the edge states near the gap are also mainly contributed from C3, C4, C5, and C6. This can be seen clearly in Figure 2e. However, unlike the case of CH, there is no dangling bond at C0 in CH_2, and thus it does not cause any localized electronic state.

In contrast, the adsorbed CH_3 pulls C1 out of the tube wall significantly, inducing the weak bonds (about 1.53 Å) around the C1 atom (shown in Figure 1c). At the same time, the local structures around C2, C3, and C4 become pyramid-like configurations. This means that the adsorbed CH_3 causes these carbon atoms to transfer from the sp^2-like to the sp^3-like hybridization. Accordingly, there exist dangling bonds at C2, C3, and C4, and these dangling bonds contribute to the local states near the Fermi level, as shown in Figure 2f.

In the case of a radical adsorbing on the DB atom in the CNT, the DB atom (C1) together with its nearest neighboring carbon atoms, C0, C2, and C3, forms a local planar configuration (Figure 1d−f). Structurally, there exist strained C−C bonds in each planar structure. These strained bonds together with the carbons in the pentagon and the octagon give rise to the defect states, narrowing the gap width of the tube significantly (Figure 3a−c). In addition, a sharp peak at about −0.6 eV (marked with A) is present in each calculated DOS, as displayed in Figure 3a−c. Further analysis reveals that these peaks originate from the carbon atoms in the pentagon. On the other hand, the different bonding behaviors of each radical at the DB atom are exhibited in the related LDOS (Figure 3d−f). For the case of CH, the DB atom of C1 is fully saturated, whereas the C0 atom remains unpaired electrons yet. As a consequence, the C0 atom contributes to large peaks at −1.6 and +1.6 eV in the calculated LDOS (Figure 3d), corresponding to the majority spin and the minority spin states, respectively. However, such unpaired electrons in C0 are fully saturated for CH_2 adsorption, thus there is no evident peak in the LDOS of C0 (Figure 3e). Distinct from both cases above, when CH_3 adsorbs on the DB atom C1, the carbon atoms of C0 and C1, together with three H atoms, form a pyramid like configuration, featuring sp^3 hybridization. On the other hand, C1 connects with three carbon atoms only, leading to the existence of the unpaired electrons on C1. Accordingly, C1 gives rise to several pronounced peaks near the Fermi level in the LDOS (Figure 3f).

From above, the defect states near the band gap are not contributed from the adsorbed radicals directly, but from the distorted structures near the adsorption sites. The induced shorter and longer bonds generate the edge states near the band, while the C atoms with unpaired electrons on the tube cause the local states near the Fermi level.

B. Vibrational Properties. Usually, the adsorption of the radical on a CNT should affect the lattice dynamics property of the tube. Meanwhile, some new vibrational modes associated with the adsorbates should appear in the vibrational spectra of the system. In this section, we employ the frozen phonon approach to explore the vibrational features of the (7,0) tube with adsorption of the radicals. To test the validity of the frozen phonon approach implanted in the Siesta package, we evaluate the vibrational frequencies of small hydrocarbon molecules, CH_4, C_2H_2, and C_2H_6, at the level of GGA-PBE. The frequencies of the symmetric C−H stretching modes are found to be 2984, 3509, and 2996 cm^{-1} for CH_4, C_2H_2, and C_2H_6, respectively, closer to those from the experiments (2917, 3374, and 2954 cm^{-1})[26,27] than those calculated at the tight-binding level (3162, 3546, and 3113 cm^{-1})[28] and at the MP2 level (3115, 3593, and 3086 cm^{-1}).[26] These results imply that the employed approach is reliable for evaluating the vibrational frequencies of the hydrocarbon systems.

Our calculations show that the stretching modes of a radical appear in the high frequency region (above 3000 cm^{-1}) and no state in the frequency region between 1700 and 3000 cm^{-1} yet. While in the frequency region below 1700 cm^{-1}, rich vibrational modes associated with C−C and C−H appear. In this frequency region, most of the vibrational features of a CNT, such as R band and G band, still remain in the cases with the adsorbates. Typically, the radial breathing mode (RBM) appears in each system, with a slight shift (less than 10 cm^{-1}) of the value of RBM frequency with respect to that of the perfect (7,0) tube (418 cm^{-1}).

To obtain the vibrational features of the radicals on the CNT, we plot the local vibrational density of states (LVDOS) for each radical on the tube in Figure 4. From Figure 4, one can see clearly that there are some peaks marked with characters in LVDOS for each radical. By examining the corresponding

TABLE 1: Typical Modes for Each Radical Adsorbing in Perfect Network of the (7,0) Tube, with the Descriptions of the Frequencies (in cm^{-1}) and the Modes[a]

system	frequency	peak	mode description	frequency	peak	mode description
CH	3203	A1	str	451	A6	swing, para
	1015	A2	ben, para	386	A7	swing, para
	978	A3	ben, para	369	A7	swing, para
	929	A4	ben, para	351	A7	swing, perp
	690	A5	ben, perp	326	A8	swing, perp
CH_2	3228	B1	str, asy	995	B6	ben, asy, in the plane
	3116	B2	str, sym	975	B7	ben, asy, out of the plane
	1425	B3	ben, sym, in the plane	961	B7	ben, asy, out of the plane
	1410	B4	ben, sym, in the plane	935	B8	ben, asy, in the plane
	1099	B5	ben, asy, in the plane	918	B8	ben, asy, out of the plane
	1095	B5	ben, sym, out of the plane	363	B9	swing, para
	1088	B5	ben, sym, out of the plane	298	B10	swing, para
	1006	B6	ben, asy, out of the plane	240	B11	swing, perp
CH_3	3140	C1	str, asy	1079	C7	ben, out of the plane
	3126	C2	str, deform	1011	C8	ben, out of the plane
	3027	C2	str, sym	1008	C8	ben, out of the plane
	1453	C3	ben, asy, out of plane	373	C9	ben, in the plane
	1421	C4	ben, asy, out of plane	367	C9	ben, in the plane
	1371	C5	umb	273	C10	swing, para
	1369	C5	umb	249	C11	swing, perp
	1108	C6	ben, out of the plane	239	C11	swing, para

[a] The third column refers to the peaks marked in Figure 4.

TABLE 2: Typical Modes for Each Radical Attaching on the DB Atom in the (7,0) Tube, with Descriptions of the Frequencies (in cm^{-1}) and the Modes[a]

system	frequency	peak	mode description	frequency	peak	mode description
CH	3223	D1	str(C−H)	738	D5	ben, para
	1715	D2	str(C−C)	290	D6	swing, perp
	898	D3	ben, perp	285	D6	swing, perp
	854	D4	ben, perp	278	D6	swing, perp
	753	D5	ben, para	116	D7	swing, para
	747	D5	ben, para	67	D8	swing, para
CH_2	3230	E1	str, asy	930	E5	ben, asy, in the plane
	3122	E2	str, sym	759	E6	ben, asy, out of the plane
	1744	E3	str(C−C)	748	E6	ben, asy, out of the plane
	1431	E4	ben, sym, in the plane	276	E7	swing,perp
	1427	E4	ben, sym, in the plane	259	E7	swing,perp
	945	E5	ben, sym, out of the plane	166	E8	swing, para
	939	E5	ben, sym, out of the plane	140	E9	swing, para
CH_3	3129	F1	str, asy	1008	F6	ben, out of the plane
	3064	F2	str, deform	997	F6	ben, out of the plane
	2950	F3	str, sym	236	F7	swing, perp
	1431	F4	ben, out of the plane	194	F8	ben, in the plane
	1430	F4	ben, out of the plane	186	F8	ben, in the plane
	1387	F5	umb	177	F8	swing, para
	1012	F6	ben, out of the plane			

[a] The third column refers to the peaks marked in Figure 6.

eigenmodes for these peaks, we identify their vibrational features, which are listed in Table 1, where, as usual, the notation for stretching (str), bending (ben), umbrella (umb), symmetry (sym), and asymmetry (asy) is used for their description. In addition, the abbreviation, para or perp, stands for the displacement of H and C atoms parallel or perpendicular to the tube axis, respectively. These notations are also used in Table 2.

In the high frequency region, as shown in Figure 4, there is only a C−H stretching mode (A1) at 3203 cm^{-1} for CH. While for CH_2, two kinds of stretching modes (B1 and B2) appear in vibrational density of states, asymmetric (3228 cm^{-1}) and symmetric (3116 cm^{-1}) modes. Unlike the cases above, the adsorbed CH_3 has three stretching modes, asymmetric (C1, 3140 cm^{-1}), deformed (C1, 3126 cm^{-1}), and symmetric (C2, 3027 cm^{-1}) modes, of which the first two modes overlap in peak C1 (Figure 4c).

In the moderate frequency region (500 to 1500 cm^{-1}), there are many kinds of bending modes (the H and C atoms in each radical displace oppositely to each other), mixing with a little twist or rocking feature. For CH, bending modes exhibit two patterns, one of which is that the displacements of the H and the C atoms are parallel to the tube axis and the other is that perpendicular to the tube axis. These modes are shown in Figure 5a,b, respectively. For the case of CH_2, there are four kinds of bending modes, symmetric or asymmetric displacements of the C and the H atoms in or out of the plane which comprises three atoms of the radical (Figure 5e−h). In fact, the modes out of the plane correspond to those with the displacements of the C and the H atoms perpendicular to the plane. Among these bending modes, it is clearly shown in Table 1 that the symmetric bending modes position at the higher frequency region than the corresponding asymmetric ones. Meanwhile, for the bending

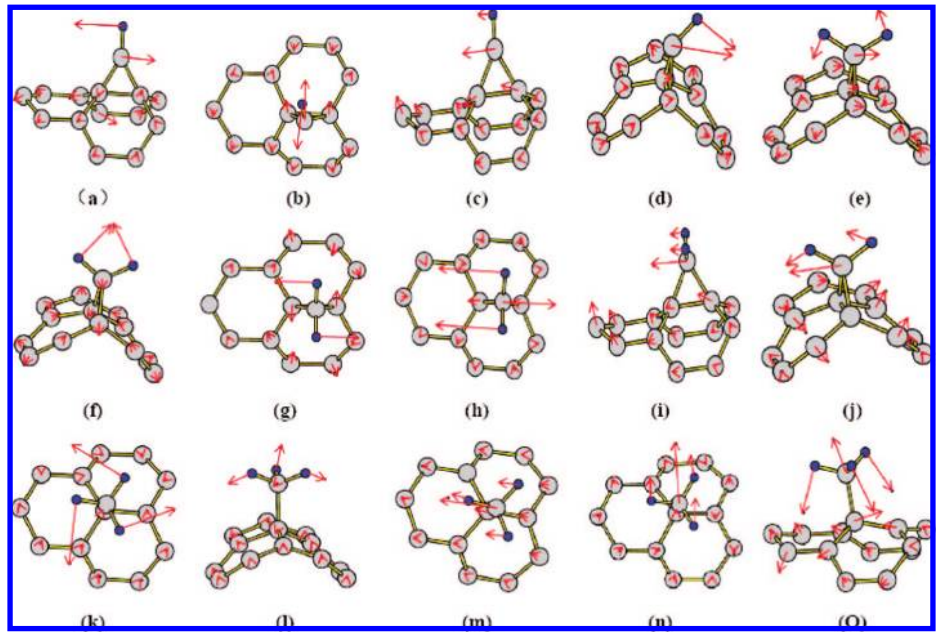

Figure 5. Typical vibrational modes for the radicals on the (7,0) tube. (a−d) for CH: bending modes (a) parallel or (b) perpendicular to the tube axis, swing modes (c) parallel or (d) perpendicular to the tube axis; (e−j) for CH_2: (e) asymmetric and (f) symmetric bending modes in the plane comprising the three atoms in the radical, (g) asymmetric and (h) symmetric bending modes out of the plane comprising the three atoms in the radical, swing modes (i) parallel or (j) perpendicular to the tube axis; (k−o) for CH_3: bending modes (k) within or (l) out of the plane comprising the three H atoms in the radical, swing modes (m) parallel or (n) perpendicular to the tube axis, (o) umbrella mode. The arrows attached at the atoms represent the direction and amplitude of the atoms displacement. The gray balls stand for the carbon atoms and the blue balls for the hydrogen atoms. No arrow attached at an atom means the displacement of this atom is very small with respect to the others.

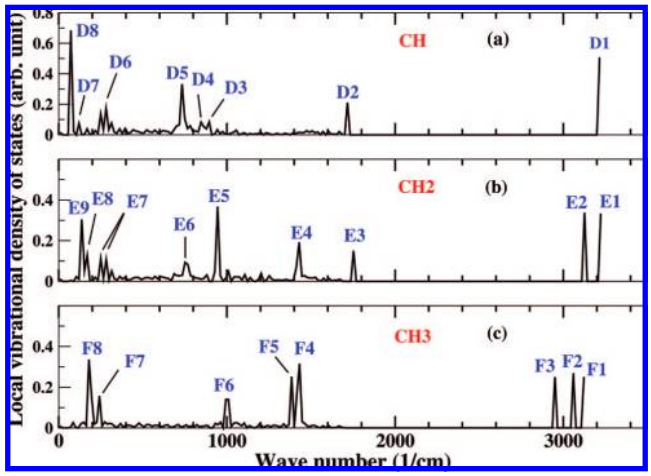

Figure 6. Local vibrational density of states for the radicals on the DB atom in the single vacancy of the (7,0) tube. Some typical peaks are marked with characters.

modes with the same symmetry, the frequencies of these in the plane are higher than those out of the plane.

In contrast, owing to the mixing with rocking or twist vibration, the bending vibrational features of CH_3 are complicated. Typically, we sort the modes to be in or out of the plane which comprises three H atoms in the radical. Here we describe these modes with the displacement of three H atoms in the plane as modes in the plane, and the others as the modes out of the plane. Comparably, the bending modes out of the plane are much more than those in the plane. Moreover, the frequencies of the former (1000−1350 cm^{-1}) are larger than those of the latter (about 370 cm^{-1}). Additionally, there is an evident umbrella like vibration at the frequency of 1371 cm^{-1}. The typical modes for CH_3 in this region are shown in Figure 5, panels k, l, and o, respectively.

In lower frequency region (below 500 cm^{-1}), we find interesting vibrational modes for each radical, which characterize the features that the C and H atoms displace from their equilibrium positions in the same direction. These modes are named as swing modes. For each radical, there are two kinds of swing modes, of which the displacements of the atoms are parallel or perpendicular to the tube axis, and the frequencies of the swing modes parallel to the tube axis emerge at a little lower frequency region than those perpendicular to the tube axis. These vibrational patterns for CH, CH_2, and CH_3 are shown in Figure 5, panels c and d, i and j, and m and n, respectively.

In addition, the vibrational frequencies of a radical adsorbed on the 5−1DB defect in the (7,0) tube are calculated, and the LVDOS for each radical is shown in Figure 6. Similar to the cases in the perfect region, some typical modes corresponding to the peaks marked in Figure 6 are identified. The features of these typical modes for each radical are described in Table 2. As a whole, the vibrational features of each radical on the DB atom are similar to those in the perfect region. As compared with the LVDOS of the perfect cases shown in Figure 4, we find two new peaks at 1715 and 1744 cm^{-1} denoted as D2 and E3 in LVDOS for the cases of CH and CH_2 in Figure 6a,b, respectively. The peak of D2 (E3) is mainly ascribed to a special stretching mode of a C−C bond. Here, the carbon atoms of the C−C bond are relevant to the carbon atom in CH (CH_2) and the DB atom in the CNT. Such a stretching mode does not appear in the vibrational density of states for the case of CH_3.

Notice that the concerned systems above contain C−H bonds. In fact, when H adsorbs on either a perfect or a defected CNT, there also exists a C−H bond. The local structure around this type of C−H bond is definitely different from those in the adsorbed radicals. For comparison, we explore the vibrational features of a H atom adsorbing at atop of a carbon atom in perfect network and on the DB atom of the defected (7,0) tube respectively. For the case of H adsorbing on the perfect tube,

the frequency of the C−H stretching mode lies at 2932 cm^{-1}, corresponding to vibrational energy of about 364 meV, which agrees well with the experimental report (360 meV).[29] In addition, two kinds of typical bending modes, parallel or perpendicular to the tube axis, are found to be at 1242 and 1191 cm^{-1}, respectively. The former corresponds to a vibrational energy of about 154 meV, being consistent with the experimental report (155 meV)[29] too. In contrast, for H adsorbing on a DB atom, the frequency of the stretching mode shifts to 3242 cm^{-1}, and those of the bending modes parallel or perpendicular to the tube axis shift downward near 1156 or 864 cm^{-1}.

Different from the cases of the radicals, the swing modes do not appear in the vibrational density of states for H adsorbed on the tube. This is mainly attributed to the different bonding environment around the C atom that bonds with H: in the case of H adsorption, the C atom connects with the other three C atoms in the CNT, whereas in the case of a radical adsorption, the connected C atom in the radical extents out from the outer wall of the tube, being more flexible for motion than that in the former case. Such flexible motion of the carbon atom is responsible for the observed swing modes.

According to the obtained results above, we propose that the concerned systems containing C−H bond(s) can be identified by the vibrational modes in high frequency regions. (1) For the radicals adsorbing on the perfect network, there are one, two, and three stretching modes, located at about 3000 cm^{-1}, for the adsorbed CH, CH_2, and CH_3 respectively. Such different numbers of the stretching modes can be used to differentiate the adsorbed radicals from each other. For the case of a H atom on the CNTs, although there is one C−H stretching mode in the high frequency region, the frequency of this stretching mode is lower by 270 cm^{-1} than that in the case of CH adsorption. According to this difference, the adsorption of a H atom or a CH radical on a CNT can be identified. (2) For the defected cases, since either CH or CH_2 adsorbing on the DB site can convert the 5−1DB defect to be a perfect network with attachment of H atom(s) at low temperatures,[19] our predicted vibrational frequencies of the CH and CH_2 adsorbed on the DB atom are hard to observe in the experiment. However, CH_3 keeps attaching at the DB site, even when the temperature of the system reaches 600 K.[19] The frequencies of the C−H stretching modes in this case shift downward by about 60 cm^{-1} with respect to those for the perfect case, which can be roughly employed to distinguish both cases.

IV. Conclusions

Based on the DFT calculation with the Perdew−Burke−Ernzerhof generalized gradient approximation, we find that the adsorbed radicals of CH, CH_2, and CH_3 can modulate the electronic structures of a carbon nanotube. Typically, for CH or CH_2 adsorption, some new edge states emerge near the band gap of the tube, and for CH_3, new local states appear near the Fermi level. Furthermore, we find some vibrational modes associated with the radicals on the CNT in our calculations, of which the values and the number of the frequencies of C−H stretching modes are dependent on the adsorbates. This can be used to differentiate the adsorbates from each other. In addition, our calculation shows that the swing modes appear in the vibrational spectrum of the CNT with adsorption of a radical but do not in that of the CNT with adsorption of a H atom. This can be ascribed to the different bonding environment around the C atom that bonds with H.

Acknowledgment. This work is partially supported by the Fund of University of Science and Technology of China, the Fund of Chinese Academy of Science, and by NSFC with code numbers of 50121202, 60444005, and 10574115. This work was partially supported by the National Basic Research Program of China, Grant No. 2006CB922000.

References and Notes

(1) Kong, J.; Franklin, N. R.; Ho, C.; Chapline, M. G.; Peng, S.; Cho, K.; Dai, H. *Science* **2000**, *287*, 622.
(2) Collins, P. G.; Bradley, K.; Ishigami, M.; Zettl, A. *Science* **2000**, *287*, 1801.
(3) Valentini, L.; Armentano, I.; Kenny, J. M.; Cantalini, C.; Lozzi, L.; Santucci, S. *Appl. Phys. Lett.* **2003**, *82*, 961.
(4) Woods, L. M.; Badescu, S. C.; Reinecke, T. L. *Phys. Rev. B* **2007**, *75*, 155415.
(5) Jhi, S. H.; Louie, S. G.; Cohen, M. L. *Phys. Rev. Lett.* **2000**, *85*, 1710.
(6) Agrawal, B. K.; Singh, V.; Pathak, A.; Srivastava, R. *Phys. Rev. B* **2007**, *75*, 195421.
(7) Gulseren, O.; Yildirim, T.; Ciraci, S. *Phys. Rev. B* **2002**, *66*, 121401(R)
(8) Zhao, J. J.; Buldum, A.; Han, J.; Lu, J. P. *Nanotechnology* **2002**, *13*, 195.
(9) Chang, H.; Lee, J. D.; Lee, S. M.; Lee, Y. H. *Appl. Phys. Lett.* **2001**, *79*, 3863.
(10) Pati, R.; Zhang, Y.; Nayak, S. K.; Ajayan, P. M. *Appl. Phys. Lett.* **2000**, *81*, 2638.
(11) Peng, S.; Cho, K. J. *Nanotechnology* **2000**, *11*, 57.
(12) Chan, S.-P.; Chen, G.; Gong, X. G.; Liu, Z.-F. *Phys. Rev. Lett.* **2001**, *87*, 205502.
(13) Chen, G.; Kawazoe, Y. *Phys. Rev. B* **2006**, *73*, 125410.
(14) Kudin, K. N.; Bettinger, H. F.; Scuseria, G. E. *Phys. Rev. B* **2001**, *63*, 045413.
(15) Park, K. A.; Choi, Y. S.; Lee, Y. H.; Kim, C. *Phys. Rev. B* **2003**, *68*, 045429.
(16) Sumanasekera, G. U.; Adu, C. K. W.; Fang, S.; Eklund, P. C. *Phys. Rev. Lett.* **2000**, *85*, 1096.
(17) Valentini, L.; Armentano, I.; Puglia, D.; Lozzi, L.; Santucci, S.; Kenny, J. M. *Thin Solid Films* **2004**, *449*, 105.
(18) He, H. Y.; Pan, B. C. *Physica E* **2008**, *40*, 542.
(19) Zhou, R. L.; He, H. Y.; Pan, B. C. *Phys. Rev. B* **2007**, *75*, 113401.
(20) (a) Sanchez-Portal, D.; Ordejon, P.; Artacho, E.; Soler, J. M. *Int. J. Quantum Chem.* **1997**, *65*, 453. (b) Troullier, N.; Martins, J. L. *Phys. Rev. B* **1991**, *43*, 1993.
(21) Perdew, J. P.; Burke, K.; Ernzerhof, M. *Phys. Rev. Lett.* **1996**, *77*, 3865.
(22) Soler, J. M.; Artacho, E.; Gale, J. D.; Garcia, A.; Junquera, J.; Ordejon, P.; Sanchez-Portal, D. *J. Phys.: Condens. Matter* **2002**, *14*, 2745, and references therein.
(23) Monkhorst, H. J.; Pack, J. D. *Phys. Rev. B* **1976**, *13*, 5188.
(24) Yin, M. T.; Cohen, M. L. *Phys. Rev. B* **1982**, *26*, 3259.
(25) Lu, A. J.; Pan, B. C. *Phys. Rev. Lett.* **2004**, *92*, 105504.
(26) Hehre, W. J.; Radom, L.; Schleyer, P. von R.; Pople, J. A. *Ab initio molecular orbital theory*; Wiley: New York, 1986.
(27) Herzberg, G. *Molecular spectra and molecular structure, Vol. 46 3. Electronic spectra and electronic structure of polyatomic molecules*; Krieger: New York, 1999.
(28) Wang, Yang.; Mak, C. H. *Chem. Phys. Lett.* **1995**, *235*, 37–46.
(29) Chiarello, G.; Maccallini, E.; Agostino, R. G.; Caruso, T.; Formoso, V.; Papagno, L.; Colavita, E.; Goldoni, A. *Phys. Rev. B* **2004**, *69*, 153409.

JP806265Q